ELSEVIER

New Astronomy 8 (2003) 777–794

New Astronomy

www.elsevier.com/locate/newast

Short-term variations of cosmic-ray intensity and flare related data in 1981–1983

H. Mavromichalaki[a,*], P. Preka-Papadema[b], I. Liritzis[c,1], B. Petropoulos[c], V. Kurt[d]

[a] *Nuclear and Particle Physics Section, Physics Department, Athens University, Pan/polis, 15771 Athens, Greece*

[b] *Astrophysics, Astronomy and Mechanics Section, Department of Physics, Athens University, Panepistimioupolis, 15783 Athens, Greece*

[c] *Research Center for Astronomy and Applied Mathematics of Athens Academy, Anagnostopoulou 14, 10673 Athens, Greece*

[d] *Institute of Nuclear Physics, Moscow State University, 119899 Vorobievy Gory, Moscow, Russia*

Received 20 February 2003; received in revised form 13 May 2003; accepted 13 May 2003
Communicated by W. Soon

Abstract

A statistical analysis of the cosmic-ray intensity (CR) daily means, registered at three Neutron Monitor stations with different cut-off rigidities (Deep River, Climax and Alma-Ata), as well as, of the solar hard X-ray flares fluence recorded by Venera-13, -14 space-probes, has been performed for the time interval 1981–1983. Various methods of time series spectrum analysis, such as Fast Fourier Analysis (FFT) and Maximum Entropy (MESA), accompanied by appropriate statistical tests, have been employed to detect periodicities, while the method of Successive Approximations (SA) is used independently in order to define the amplitude and the phase of each fluctuation. New short-term periodicities of 100, 70, 50 and 32 days, in addition to the known ones of 152, 27 and 14 days, appeared in cosmic ray data. During this particular time interval, similar spectral behaviour has been reported in the solar hard X-ray flares data. The influence of the solar hard X-ray flares variability in the energy range 50–500 keV, expressed by their fluence values, upon the cosmic-ray modulation, is discussed.

PACS: 96.60.Tf; 96.60.Rd; 96.40.-z; 96.40.Kk
Keywords: Sun: flares; Methods: miscellaneous; Cosmic rays; Sunspots; X-rays: general

1. Introduction

The intensity of galactic cosmic-rays (GCR) is assumed to be essentially constant outside the heliosphere. The main characteristic of cosmic-rays observed inside the solar cavity is the time variability on a wide range of time scales. The cosmic-ray particles provide an indirect measurement of the global structure of the interplanetary magnetic field (IMF), since they sample a large volume of the solar cavity in their travels from its boundary to the Earth. The temporal changes observed must be due to the interaction of cosmic-ray particles with the IMF that is carried by the solar wind (Cane et al., 1998). The problem is to find out the pattern of the interplanetary magnetic field and its flow, to determine the time

*Corresponding author.
E-mail addresses: enavromi@cc.uoa.gr (H. Mavromichalaki), ppreka@cc.uoa.gr (P. Preka-Papadema), liritzis@rhodes.aegean.gr (I. Liritzis), vpetrop@academyofathens.gr (B. Petropoulos), vgk@srol.sinp.msu.ru (V. Kurt).
[1] Laboratory of Archaeometry, Department of Mediterranean Studies, University of the Aegean, Rhodes 85100, Greece.

1384-1076/03/$ – see front matter
doi:10.1016/S1384-1076(03)00066-6

and spatial evolution of their configurations and to relate them to cosmic-ray variations.

Analysis of cosmic-ray intensity time evolution covering over four solar cycles has led to the identification of intensity variations with several periodicities, most of them correlated with different solar phenomena. Dorman and Ptuskin (1981) have proposed that the possible natural large-scale pulsations of the heliosphere are probably the origin of a new type of cosmic-ray variation with characteristic periods varying from 1 to 2 years to tens of years. Attolini et al. (1987) have applied their statistical technique of cyclograms to the Climax Neutron Monitor station, and they also studied the cosmic-ray intensity variations in the periodicity range of 1 to 10 years, where the 2-year variation was clearly observed.

Okhlopkov et al. (1986) have studied the cosmic-ray variations at different isobaric levels and have revealed a new kind of galactic cosmic-ray zonal modulation. The frequency structure of the cosmic-ray variations has presented significant peaks with periods of about 2, 1.5, 1, 0.75 and 0.5 years. Xanthakis et al. (1989) analyzing time series of seven Neutron Monitor stations into trigonometric series for the time interval 1964–1985 determined two kinds of periodicities appeared in these data: long-term occurrences at periods greater than two years (10.41, 8.41 and 5.50 years) which differed very little in amplitude from station to station, but were similar in phase, as well as, short-term variations smaller than two years (2, 1, 0.7 and 0.5 years), which were also similar in all stations but appeared in variable time intervals.

Later, Kudela et al. (1991) noted that there are two distinct regions of cosmic-ray periods, with a limit of 20 months (1.68 years) between them, caused by different physical mechanisms. The large-scale variations are caused by the solar cavity dynamics, whereas the short-scale ones by transient effects in interplanetary space. This depends on the fact that the short time periods have different probability of occurrence in different epochs. Valdés-Galicia et al. (1996) and Valdés-Galicia and Mendoza (1998) have reported on a short-time variation of 1.68 yr in the cosmic-ray intensity observed at the Earth in the neutron monitor range of energies (several GeV). They proposed that this cosmic-ray variation might appear as a consequence of phenomena rooted in the solar interior and could help in understanding the origin of the solar magnetic cycle. According to Antalova (1997), these phenomena are related to the magnetic flux emergence and transport. On the other hand, the cosmic-ray intensity observed at the Earth's surface is modulated by the solar activity expressed by different parameters (Forbush, 1958).

As the solar flares are the most energetic events on the Sun, they provide the unique opportunity for studying the energy release and acceleration of charged particles. Some of the most powerful flares are strong sources of high-energy particles that have been detected soon after the flare as fluxes of energy particles at the top of the atmosphere.

Thus, studying the soft or hard X-ray and gamma-ray solar flares we can conclude about their influence on cosmic-ray solar modulation (Longair, 1992) due to the close relation between them and the global changes in the Sun's magnetic field that affect the IMF variations (Cane et al., 1999).

For the maximum phase of solar cycle 20, cross-correlation analyses between Calgary Neutron Monitor data and soft (1–8 Å) X-ray parameters did not reveal a clear role for long duration soft X-ray flares (LDE-type flares) in GCR modulation (Storini et al., 1995). Jakimiec et al. (1997) have considered the possibility that non-stationary random processes may influence the cosmic-ray and X-parameters relationship and mask the LDE role. To the contrary, Antalova (1994) reported that the long-duration events (LDE), which precede the formation of coronal holes during the 20th and 21st cycles, among the significant periodicities, exhibit that of 1.6 yr, which is the recent established period of cosmic-rays. McIntosh (1992), also, found that the total area of coronal holes shows a 1.62 ± 0.14 yr variation during the period 1977–89. These findings indicate a close link between LDE-type flares or coronal holes with magnetic flux emergence and transport, and present variations similar to that of the reported cosmic-ray fluctuation.

In this work, the role of the solar flares in the cosmic-ray intensity variability is investigated, using the hard X-ray emission in the energy range 50–500 keV as a mark of flare production with high enough energy release accompanied by strong variations in the solar magnetic field. For this purpose an attempt

is made to determine the smaller than 20 months cosmic-ray short-term variations and to correlate them with those of the hard X-ray solar flares. Moreover the examined 1981–1983 interval is a period of particular importance, due to the emergence of a great number of solar flares.

2. Data presentation

It is known that a different behaviour is reported between the sunspot numbers—a commonly used tracer of solar activity—as well as, the solar flare index, for the full disk of the Sun that gives the total energy emitted by the flares (Kleczek, 1952; Atac, 1987) around the maximum epochs of 21st and 22nd solar cycles. During 21st solar cycle the solar flare index was high between 1979 and 1982 becoming slightly higher in 1982, while the sunspot number was at maximum in 1979 (Fig. 1). This strong flare activity during 1981–1983 is associated with other activities, such as, coronal mass ejections (CMEs), interplanetary shock waves, intensity of interplanetary magnetic field (IMF) and high-speed solar wind streams at 1 AU. All these activities present the same trends for this time period (Webb and Howard, 1994; Smith, 1990; Schwenn, 1983; Nakai and Kamide, 1994; Mavromichalaki et al., 1988).

On the contrary, Ozgüc and Atac (1994) showed that during solar maximum of the 22nd cycle both annual mean sunspot numbers and the solar flare index values were comparable. Moreover, Mavromichalaki et al. (1995) have shown that during the 21st solar cycle, the solar H_{α} flares ($>$1B) and not

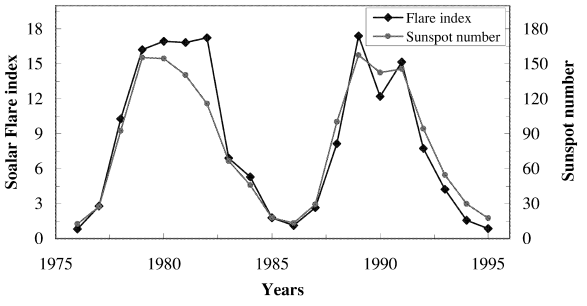

Fig. 1. Yearly values of the sunspot number and the solar flare index for the time interval 1975–1995 (solar cycles 21 and 22).

the sunspot number affected mainly the cosmic ray modulation, in contrast with the 20th solar cycle. Storini et al. (1995) underlined that the sunspot number is not the right index for solar induced effects in the interplanetary medium for the cycles 20 and 21. A large cosmic-ray intensity depression with an amplitude of 16–22% was observed at 13–14 July 1982, by the world-wide network of cosmic-ray detectors (lower panel of Figs. 2 and 3). This depression identified as a typical Forbush decrease large amplitude represented a great interest (Mavromichalaki et al., 1991).

Rieger et al. (1984) noted that the greatest energetic photon flare activity occurred in June/July and November/December 1982, as we can also see in the occurrence rate of hard X-ray solar flares with energy upper than 50 and 150 keV (Fig. 2(b) and 2(c)) that have been recorded by SMM and Venera 13, 14 space probes (Liritzis et al., 2001). The cosmic-ray intensity from Alma-Ata neutron monitor station also presented in Fig. 2(d), shows clearly an inverse relationship with the occurrence rate of the solar flares (Forbush, 1958) indicating the two corresponding decreases. Analogous behaviour appears in Climax and Deep River cosmic-ray data.

In this study, the problem of the galactic cosmic-ray modulation by solar flares with high enough energy release is investigated. Barat et al. (1987), using hard X-ray flares measured onboard Venera-13, -14, calculated the actual measured fluence (energy release per burst) over the total burst duration, for events with energy upper than 50 and 150 keV.

The sum of the fluence per second for all the events during a day expresses the energy emitted by the daily number of hard X-ray solar flares per second. Based on this aspect, two time series for events with energy upper than 50 keV (referred hereafter as time series F50) and that with energy upper than 150 keV (referred hereafter as time series F150) were studied.

The last one has been smoothed into weekly values for the purpose of our statistical analysis in order not to have gaps over the entire analyzed period. These time series are presented in Figs. 3 and 2a, respectively. In addition, the occurrence rate of hard X-ray flares recorded by Venera-13, -14 and SMM (Solar Maximum Mission) space probes has been used (Liritzis et al., 2001). Both missions have

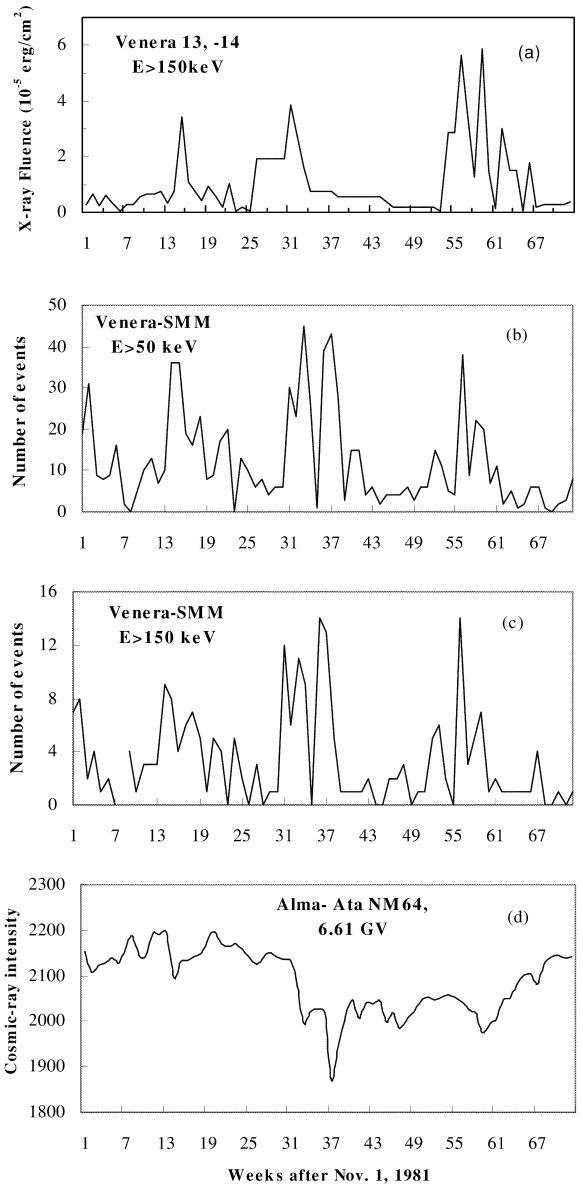

Fig. 2. Weekly values of the F150 time series are given in (a). The occurrence rate of hard X-ray solar flares with energy upper than 50 keV and upper than 150 keV measured by Venera-13 and -14 and SMM space probes are presented in (b) and (c), respectively. The cosmic-ray intensity from Alma-Ata Neutron-Monitor station is also showed in (d).

a common time interval, i.e. from November 1981 until March 1983.

In order to investigate the existence of short-term variations in cosmic-ray intensity and compare them

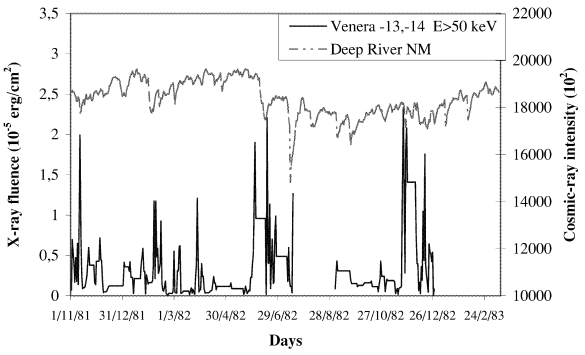

Fig. 3. Daily values of the cosmic-ray intensity from Deep River Neutron Monitor station (top) and F50 time series (bottom) from November 1, 1981 to March 13, 1983.

with the ones of the above time series, daily corrected for pressure values of the Deep River (cut-off rigidity 1.02 GV), Climax (cut-off rigidity 2.96 GV) and Alma-Ata (cut-off rigidity 6.61 GV) Neutron Monitor stations have been used. We note that although the network of neutron monitors contains an extended data bank, it is the common time interval between SMM and Venera missions that provided the hard X-ray data examined in this work.

3. Statistical analysis and results

All these data sets have been subjected to spectral analysis. In the frequency domain two different spectral analysis techniques, Fast Fourier Transformation (FFT) and Maximum Entropy Spectrum Analysis (MESA) have been used, details of which are given elsewhere (Liritzis et al., 1994, 1999). Both the autocovariance MESA and FFT methods see the data through a pre-selected fixed window and require the unrealistic assumption of a periodic or a small extension outside the observed record.

For the FFT method, the significant levels of the obtained periods derive from the cumulative periodogram of the cumulative sums of Fourier coefficients at 75 and 95% levels, following the Kolmogorov–Smirnov test for a uniform distribution of ordinates, i.e. a plot of the cumulative frequencies of the power spectrum density against frequency (Saporta, 1990).

As for MESA, the whole time series was truncated

in both ends producing subsets of variable length. The stability and regularity of the obtained periodic terms was studied in a time-evolutionary way. The peak stability has been also checked with the application of various filter lengths (orders of autoregressive process). As a rule, the Berryman criterion (Berryman, 1978) has been applied for the selection of the best filter length (F), in which $F = 2N/\ln 2N$, where N is the number of data points. The most appropriate filters F are those that do not provide spurious peaks by a splitting process (over-smoothing) or by producing broad spectrum (under-smoothing). Due to the above unresolved issues, the errors attached to the obtained periods are the full width at half maximum (FWHM) of each peak as well as the peak shift due to filter effect and subset analysis.

In the time-phase domain the method of Successive Approximations (SA) was applied. This method introduced by Xanthakis and his colleagues have been satisfactorily used in various continuous and non-continuous time-series (Xanthakis et al., 1989, 1995, etc.). The observed time series are fitted by a sum of sinusoidal waves in order to find an analytical expression consisting of a network of quasi-periods and computing their amplitude and phases. It provides analytical representation of the total record and locates the periods in the time domain. Liritzis et al. (1999) have developed, for the first time, a software for the SA method.

The basic idea of the method is the following: The best fit of the time series is made in order to find long-term quasi-periods. Therefore, the number of calculating values per time interval (A^{cal}) is given by the following relation:

$$A^{\mathrm{cal}} = a_o + \sum_{i=1}^{n} a_i \sin[\,(2\pi/T_i)(T - Ts)] \qquad (1)$$

where: $Ts < T < Te$, Ts and Te are the start and end time-terms of each calculated quasi-period, a_0 is the constant shift of the curve, a_i the amplitude of the i-sinusoidal curve (positive or negative value means that the curve is above or below the constant shift) and T_i is the ith periodicity.

The computed values are subtracted from the observed ones and the residuals are fitted by a similar relation in order to be identified as medium quasi-periods and to produce new residuals. The latter ones are fitted by an analogous relation to be identified as smaller quasi-periods and final residuals. The last calculated time series (A^{cal}) summarizes all the previous results. The standard deviation (σ) as well as the accuracy of our computations (Ac) are checked step by step insuring the validity of the results.

The simultaneous application of these different methods of spectral analysis is ideally expected to produce similar periods, independently of the particular properties of the methods. However, due to slight differences in the techniques used to determine the harmonic frequencies, these methods are used as a complementary way that offer a check upon computational accuracy and stability, frequency and power spectral density and allows careful scrutiny of the periods of interest and reasonable determination of the actual periods present. The rule of $P < N/3$, where P is the obtained periodicity and N is the number of data points, is considered as an acceptable criterion for evaluation of existing periodic terms in our analysis (Chatfield, 1984).

Fig. 4 shows the comparative study first applied to the F50 time series. Prior to the analysis this time series was smoothed by a 3-terms moving average, then it was detrended with the subtraction of a third order polynomial. The non-random nature of this time series was estimated through the application of randomness test.

Periodicities at 154 ± 50, 67 ± 15, 40 ± 5, 24 ± 3, 17 ± 2, and 12 ± 1 days were derived from FFT spectrum analysis (left panels of Fig. 4). The Kolmogorov–Smirnov test of the integrated periodogram has been used to evaluate the most significant frequency cycles at 75 and 95% accuracy. Significant levels at higher than 95% confidence level were found, although the higher period inheres a large variability.

Subsequently, the F150 time-series were smoothed by a 5-terms moving average, a satisfactory smoothing, presenting low and high frequency components, followed by detrending and subtraction of a first-order polynomial. As a result of this smoothing, the smaller terms were removed. The FFT have shown periodicities at 174 ± 60, 100 ± 10, 63 ± 6, 41 ± 3 and 28 ± 3 day with a confidence level $>95\%$, according to the Kolmogorov–Smirnov test (right panels of Fig. 4). Although the higher period has a large

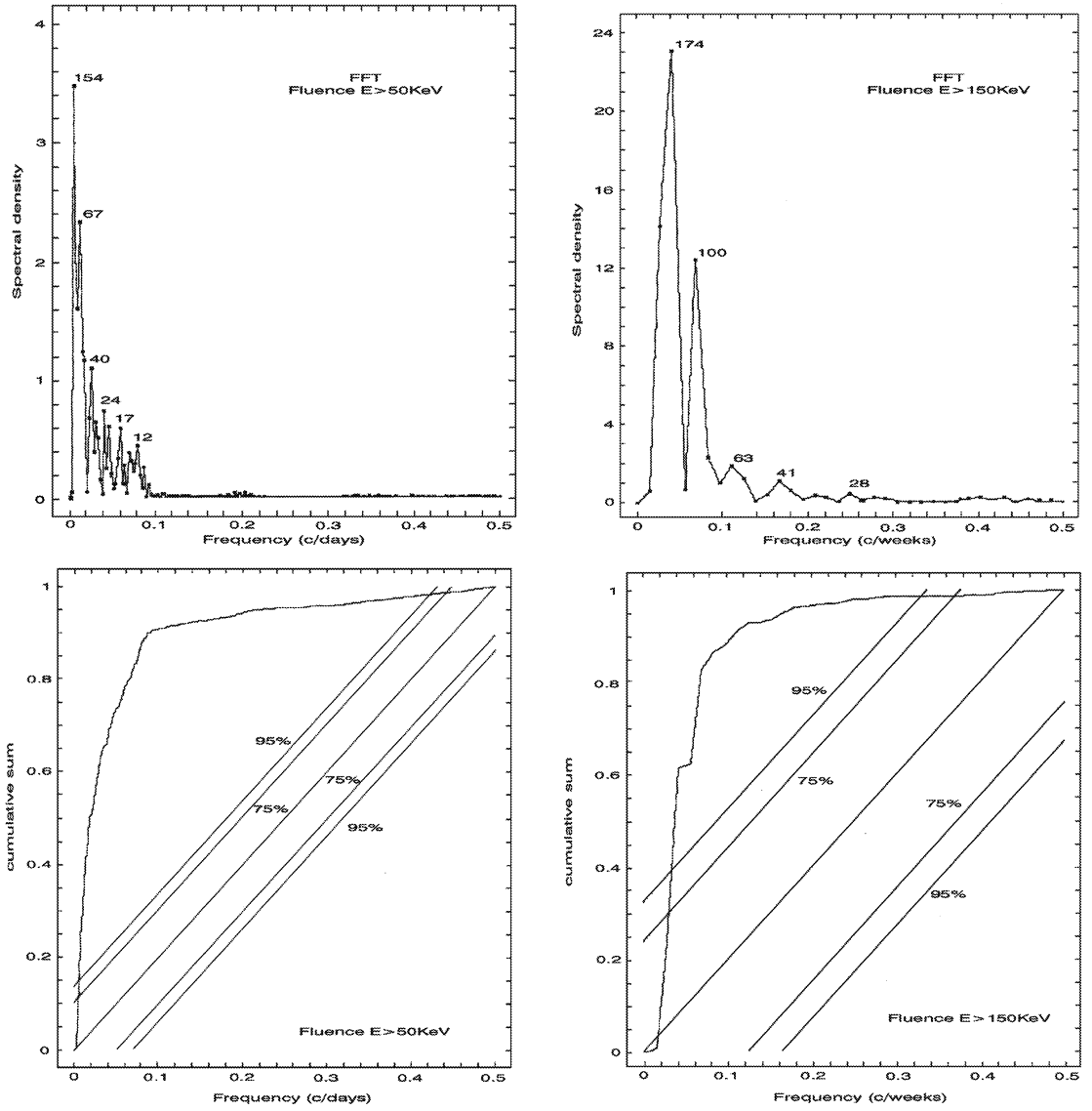

Fig. 4. FFT analysis of the F50 time series (upper left) and the F150 time series (upper right) with the corresponding Kolmogorov–Smirnov tests (lower panels). This is an integrated periodogram of the cumulative sum of Fourier frequency coefficients and the two parallel lines on both sides of the diagonal represents the 75% (inner) and 95% (outer) significance level of respective summed frequencies in the integrated periodogram curve.

variability, a trend of the time series is expressed by this term. In the undetrended series the presence of low frequencies, in the range below 30 days, have been found to be of low significance, because of the short data interval (1 week per point), that is near to the Nyquist limit (1 cycle per 2 weeks), and as a result of the smoothing and detrending procedures.

An example of MESA computations applied to the

F50 time-series for filter length $F = 84$ and $F = 94$ is presented in Fig. 5 (two upper panels). The suitable filter range is $F = 28$–99. We note that the periodicities of 25 ± 3, 18 ± 2, 12 ± 1 and 8 ± 1 days have the strongest peaks in all the subsets and filters, while the one of 100 ± 25 days is occasionally shifted into periodicities of 52 ± 5 and 67 ± 15 days.

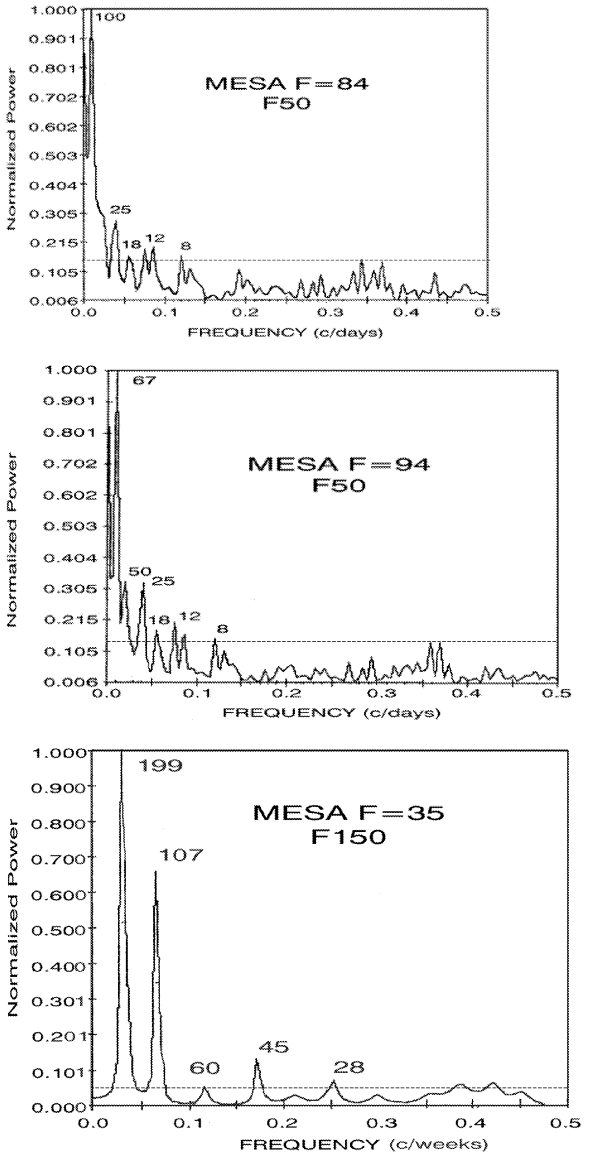

Fig. 5. The power spectrum of the F50 time series and F150 times-series computed by the MESA analysis. The spectrum relates to the detrended time series total record for two filter lengths, $F = 84$ and $F = 94$ for the F50 and F = 35 for the F150 time series.

Also, an example of MESA computations applied to the F150 time-series for $F = 35$ is presented in Fig. 5 (bottom panel). The suitable filter range is $F = 7$–39. We note that, in all the subsets and filters, the periodicities of 199 ± 36 and 107 ± 9 days have the strongest peaks, while those of 60 ± 3, 45 ± 5 and 28 ± 2 days appear sporadically. The higher of them represents a trend of the time series. The dashed horizontal lines in Fig. 5 show the σ level (68%) of the confidence of the spectral density estimated by the procedure using by Maravilla et al. (2001).

A sequence of peaks at 140 ± 14, 88 ± 10, 50 ± 4, 32 ± 2, 27 ± 2 days is outlined from the FFT analysis of cosmic-ray data (Fig. 6). A Kolmogorov–Smirnov test gives all these obtained periods with a significance level greater than 95%. It is interesting to note that the periodogram of the FFT analysis of cosmic-ray intensity (Fig. 6) and the one of F150 time series (right panels of Fig. 4), both on a weekly basis, exhibit a characteristic similar behaviour.

The SA method was applied on the F50 and F150 time series as well as on the cosmic–ray intensity daily values (referred hereafter as CR time series). Successive 'representation' of the observed time series using this method is shown in the Figs. 7–9, respectively. The analytical expressions for all the time series as well as the calculated amplitude and phase of each found quasi-period are given in Tables 1–3. It is noted that the periods in the sine functions of the F150 time series, used for the SA fitting, are integer numbers of weeks but are quoted in days in order for easy comparison with similar results given by the other time series. The figures outline that the observed values are in satisfactory agreement with the calculated ones, by the above analytical expressions. This last point also emerges from the standard deviation (and the accuracy) between observed and calculated values.

Analytically, the quasi-periods obtained by all successive approximation steps, as well as, their respective standard deviation (σ) and accuracy (Ac) for the F50, F150 and CR time series are given in Table 4. Quasi-periods at 160, 70, 50, 32, 26, 21, 16,

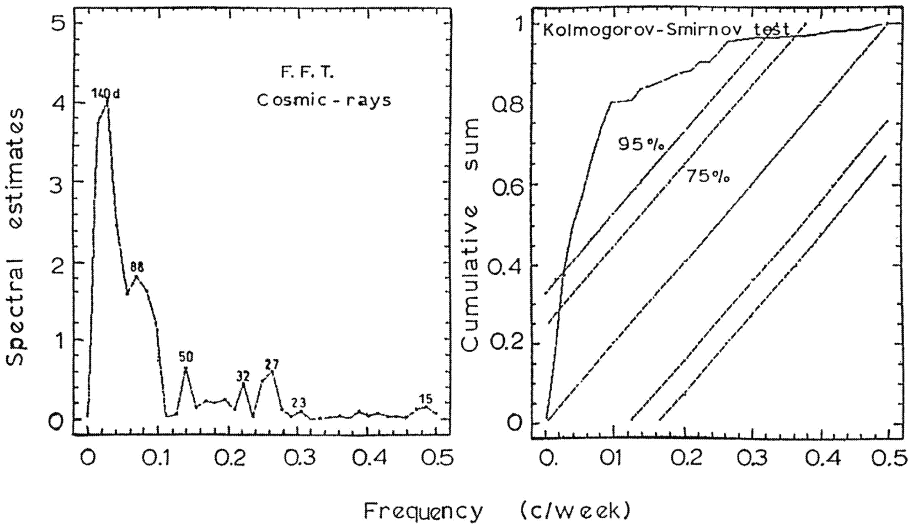

Fig. 6. FFT analysis of the cosmic-ray time series with the corresponding Kolmogorov–Smirnov test. This is an integrated periodogram of the cumulative sum of Fourier frequency coefficients and the two parallel lines on both sides of the diagonal represents the 75% (inner) and 95% (outer) significance level of respective summed frequencies in the integrated periodogram curve.

10 and 5 days for the first time series (F50,) as well as at 168, 98, 70, 42, 28 and 21 days for the second one (F150) and 130, 100, 70, 50, 32, 24, 16, 10 and 5 days for the third one (CR) were found. The accuracy of our results is 68, 71 and 99%, respectively and the associated error is considered as ± 2 days, except of the F150 time-series where it is ± 2 weeks. It is noted that the quasi-periods of 160 and 168 days express a trend of the corresponding time series. Although the method of SA does not provide a satisfactory accuracy between observed and calculated values by the analytical expressions given in Tables 1–3, the periods are in agreement with the periodicities calculated by the other methods (see Table 5).

The period of 100 days is not clearly defined by FFT method due to the large width of the peaks at about 152 and 70–80 days. On similar grounds, the period of 70 days in the CR time series analysis is contained in the large spread of the peak at 88 days. Moreover, for the F50 and F150 time series analysis a shift exists in the 32 days spectrum peak to 40–42 days, and the period of 50 days is poorly defined due to the large spread of its neighboring peaks. The presence of high frequencies—in the range below to 27 days—have been found to be of low significance and/or as a result of being smoothing and detrending procedures.

The simultaneous application of these spectral methods of analysis gives similar periods on cosmic-rays and solar flare records. All individual periodicities obtained in this work along with their uncertainties are given in Table 5. The apparent differences in exact peak values in the spectra are essentially similar, within their errors. The lower frequency peaks represent complete sine oscillations or trends. For a comparison the results of the statistical analysis on the occurrence rate time series of hard X-ray flares with energy upper than 50 and 150 keV which have been recorded by SMM and Venera 13, 14 space-probes during the time interval 1981–1983, is also presented (Liritzis et al., 2001).

4. Discussion

From the employed spectral methods of analysis the following groups of periodicities appeared in our data series, such as in the galactic cosmic-rays, as well as, in the solar activity data, are obtained (Table 5):

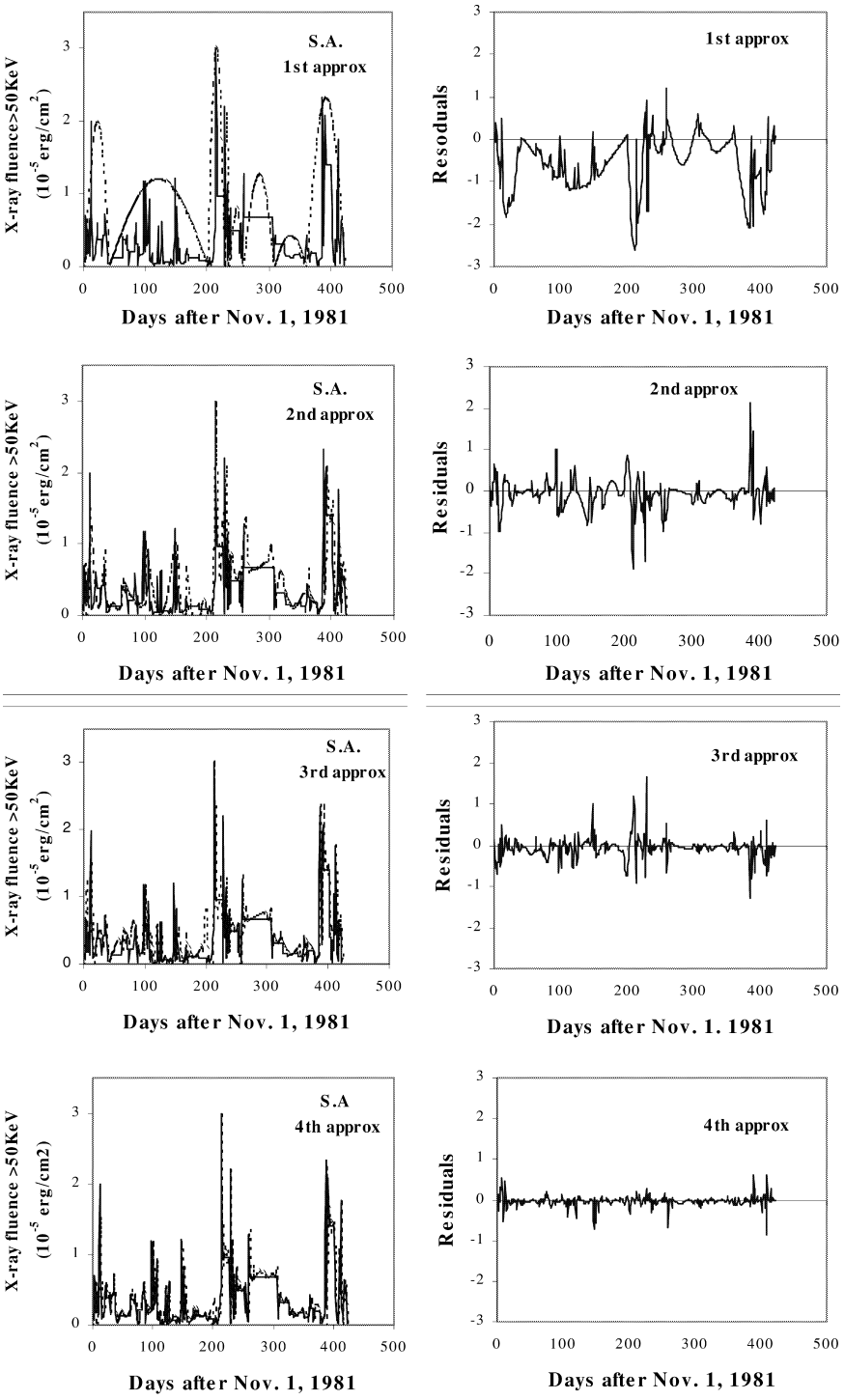

Fig. 7. Results of the SA method on the F50 time series. The curves of the analytical expressions of the computed quasi-periods (1st, 2nd, 3rd and 4th approximation, respectively) compared with the observed time series (left panels) as well as the corresponding residuals (right panels) are presented. The final curve consisting of all the quasi-periods and the last residuals are presented in the bottom panel. The accuracy of the results is 98%.

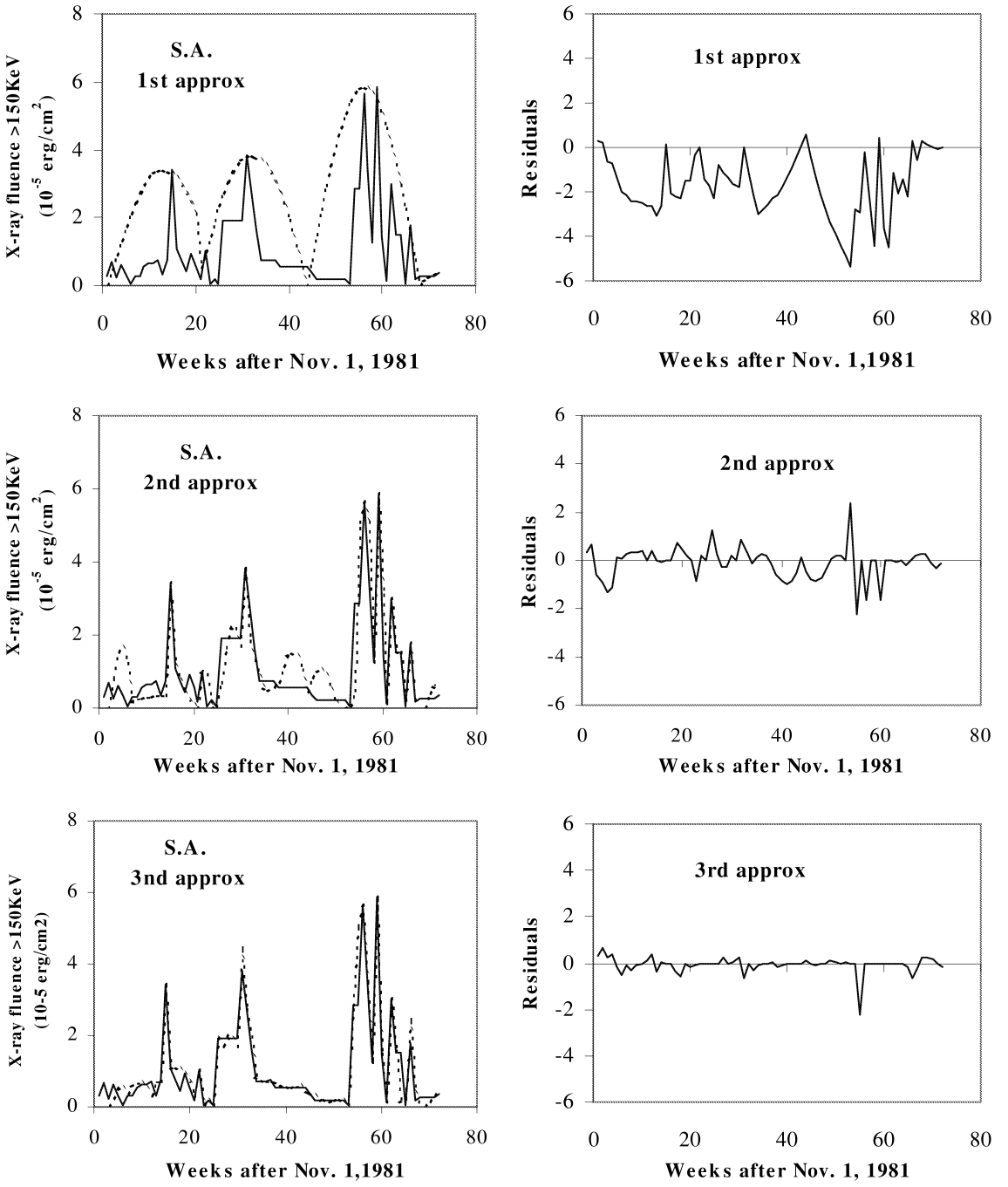

Fig. 8. Results of SA method on the F150 time series. In the three panels are presented the curves of the analytical expressions of the computed quasi-periods (1st, 2nd and 3rd approximation) compared with the observed time series, (left panels) as well as the corresponding residuals (right panels) are given. The final curve consisting of all the quasi-periods and the last residuals are presented in the bottom panel. The accuracy of the results is 71%.

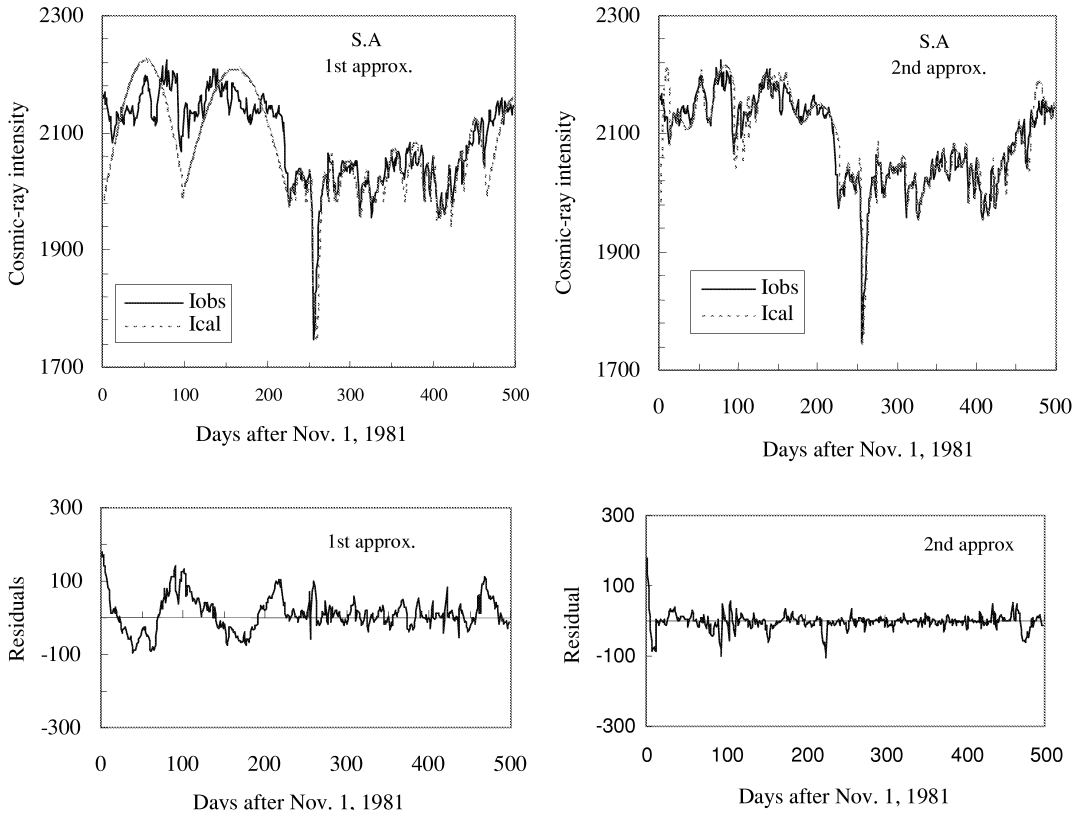

Fig. 9. Results of SA method on the CR time series. The curves of the analytical expressions of the computed quasi-periods (1st and 2nd approximation) compared with the observed time series (left panels) as well as the corresponding residuals (right panels) are given. The final curve consisting of all the quasi-periods and the last residuals are presented in the bottom panel. The accuracy of the results is 99%.

152 days, 100 days, 70 days, 50 days, 32 days, 27 days and 14 days

We note that the results of SA method are compatible with those of the other methods. Moreover, SA gives the opportunity to reproduce the observed time-series by an analytical relation fitted by some sinusoidal curves, as well as, to define the phase and the amplitude of each found quasi-period.

It is known that the periodicity of 27 days is due to differential rotation of the Sun and the one of 14 days is a quasi-period of this peak. According to Kudela et al. (1991) the variation of 27 days in cosmic-ray data reveals a complex structure during the solar activity maxima 1969, 1981 and 1989. The peak corresponding above 27 days shows a wider and double peaked structure in the spectra for solar activity maximum years (1969 and 1981), while only single peak pattern appears for the sunspot minimum years. It is the most stable period whereas the higher frequencies, corresponding to periodicities of several days, exhibit the power spectra with a complex structure for different epochs due to a combination of different transient effects with unstable periodicities growing and decaying throughout the entire period of observations.

The quasi-periodical variations of the cosmic-ray intensity with a period of about 13 days have been also studied in the data recorded through ionization chambers at Huancayo and at Cheltenham–Fredericksburg during the solar cycles 18, 19 and 20. The amplitude of this oscillation was in negative correlation with the Zürich sunspot number (Filisetti and Musino, 1982). For the cycles 18 and 19, these amplitudes present, like of 27-day oscillation, two maxima, while for the cycle 20 there is only one

Table 1
Analytical expression of F50 time series as a function of quasi-periods (in days)

$$A^{cal} = a_1 \sin[(2\pi/160)(T - Ts)] + a_2 \sin[(2\pi/70)(T - Ts)] + a_3 \sin[(2\pi/50)(T - Ts)] + a_4 \sin[(2\pi/32)(T - Ts)] + a_5 \sin[(2\pi/26)(T - Ts)] + a_6 \sin[(2\pi/21)(T - Ts)] + a_7 \sin[(2\pi/16)(T - Ts)] + a_8 \sin[(2\pi/10)(T - Ts)] + a_9 sin[(2\pi/5)(T - Ts)],$$

where $Ts < T < Te$, Ts (start time) and Te (end time) express the number of days after 1/11/81

		Ts	Te			Ts	Te
a_1	1.213	40	200	a_8	0.150	132	145
a_2	−0.956	63	100		1.188	254	266
	2.331	360	423		0.590	298	308
a_3	0.433	308	360		−0.920	391	401
	1.268	258	308		0.049	90	96
	−1.199	100	148		0.116	154	166
	−2.087	363	387		0.090	366	378
	1.995	1	40		0.343	202	208
a_4	0.059	265	298		−1.760	401	412
	−0.598	266	298		−1.965	214	224
	−0.817	132	148		−0.312	242	352
	−0.378	48	63		0.636	1	10
a_5	3.000	200	228		0.395	20	30
	−0.597	166	192		0.032	64	74
	−0.317	324	350		0.000	242	252
	0.041	326	352		−0.287	312	322
	0.316	350	363		0.219	102	107
	−1.822	12	35		0.002	310	320
a_6	0.803	236	258		0.057	368	378
	0.265	172	194		−1.156	4	12
	−0.905	151	166		0.026	40	48
	0.054	264	284		0.090	192	200
a_7	0.003	330	348		0.577	234	242
	0.381	308	324		−0.970	12	20
	0.264	48	64		0.016	40	48
	−2.603	200	214		−0.269	352	360
	0.421	74	88		−0.715	1	8
	0.853	194	208		0.010	40	48
	−0.236	48	62		0.067	88	96
	−0.421	70	84		−0.172	186	194
	0.013	172	186		−0.742	194	202
	−0.101	284	298		0.000	242	250
a_9	−0.308	298	305	a_9	0.996	145	150
	0.065	353	360		0.291	216	221
	0.910	224	230		−0.164	348	353
	0.309	417	423		−0.493	403	408
	−0.365	30	36		0.388	1	4
	0.518	116	122		0.132	36	40
	0.598	122	128		−0.021	128	132
	−0.420	166	172		−0.764	150	154
	−1.876	208	214		−0.810	214	218

Table 1. Continued

	Ts	Te		Ts	Te
0.483	218	224	−0.770	224	228
−0.989	254	260	−1.687	228	230
0.089	394	400	−0.375	238	242
0.593	404	410	0.235	308	312
0.252	14	20	−0.021	322	326
−0.140	64	70	−0.421	360	364
−0.254	154	160	−0.782	400	404
0.047	160	166	0.541	410	414
0.013	298	304	0.176	30	34
−0.134	324	330	0.053	112	116
2.207	228	233	−0.563	116	120
−0.317	35	40	−0.493	122	126
−2.030	387	391	−0.006	128	132
−0.763	412	417	0.096	168	172
−0.632	101	106	1.187	208	212
−0.505	106	111	−0.342	221	225
−0.317	111	116	−0.160	229	233
−0.715	260	265	−0.166	250	254
2.145	384	389	0.153	254	258
−0.128	23	28	−0.159	320	324
			0.012	396	400

clear maximum. The period of 14 days is also appeared in our analysis in weekly data (Table 5).

Various authors have already reported periodicities from 154 to 27 days on solar activity data. To our knowledge, the existence of the short-term periodicities of 70, 50 and 32 days are recorded in cosmic ray data for first time, in contrast to the solar activity parameters in which they are known. The period of 100 days is in agreement to earlier results. Xanthakis et al. (1989) found the periods of 4 and 3 months on the monthly distribution of cosmic-ray intensity registered by six Neutron Monitor Stations during the period 1964–1985. The periods of 2.7 and 3.7 months have also been reported in cosmic-ray intensity for the 21st cycle (Mavromichalaki et al., 1989), and neutrino Homestake data analysis (Liritzis, 1994).

The periodicity of about 154 days was first found in gamma-ray and soft X-ray flares data, obtained from February 1979 till September 1983 by Rieger et al. (1984). Most of other studies on solar flare data indicate a period near 154 days, but it appears to be dominant in cycle 21, especially in the time interval 1978 to 1983 corresponding to the solar activity maximum (Bogart and Bai, 1985; Ichimoto et al., 1985 etc). Evidence for a periodicity of 154 days has

Table 2
Analytical expression of F150 time series as a function of quasi-periods (in days)

$$A^{cal} = 2 + a_1 \sin[(2\pi/168)(T - Ts)] + a_2 \sin[(2\pi/98)(T - Ts)] + a_3 \sin[(2\pi/70)(T - Ts)] + a_4 \sin[(2\pi/42)(T - Ts)] + a_5 \sin[(2\pi/28)(T - Ts)] + a_6 \sin[(2\pi/21)(T - Ts)],$$

where $Ts < T < Te$, Ts (start time) and Te (end time) express the number of weeks after 1/11/81

		Ts	Te
a_1	3.420	1	20
	3.830	20	44
	5.850	44	68
a_2	−1.090	6	14
a_3	2.550	38	48
	−3.355	48	54
	2.260	66	72
a_4	0.360	68	72
	2.234	1	6
	−0.970	32	38
	−1.314	1	6
	0.402	6	12
	0.712	16	22
	−0.979	38	44
	−0.827	44	50
a_5	−0.283	16	20
	2.029	20	24
	0.891	26	30
	1.810	54	57
	0.890	30	34
	0.253	34	38
	0.932	65	69
a_6	0.422	12	15
	−0.278	27	30
	0.324	50	53
	−0.333	69	72

also been found in nonflare indices of solar activity as sunspot number, the Ottawa 10.7 cm quiet-Sun flux, etc. (Ichimoto et al., 1985; Kile and Cliver, 1991). Although many authors mentioned that this periodicity is strongest for cycle 21 it does not appear in the power spectrum of solar 1–8 Å X-ray index for the interval 1977–1981 performed by Ozgüc (1989), but it does appear around 78 days.

Moreover, Valdés-Galicia et al. (1996) have reported that the periodicity of 154 days (5.1 months) is appeared during solar cycle 21 and not in cycle 20, in the power spectral density of cosmic-ray intensity registered at Deep River Neutron Monitor. Also the evidence for the 154-day periodicity in flare-related data and cosmic-ray intensity is convincing for the interval 1978–1983 characterized by strong flare activity (Mavromichalaki et al., 1990).

Bai and Cliver (1990) underlined that there are cases where a periodicity is seen to disappear for a long interval and then to appear at the same phase or 180 degrees out of space and an example of this effect is the 155-day periodicity. Rybak et al. (2000) as well as Antalova et al. (2000) noted the intermittent character of the 150-day solar periodicity in the 20, 21 and 22 cycles for solar soft X-ray parameters, while the power of the 155-day periodicity of solar SXR data is remarkably better during the 21st than in the 20th cycle. Cane et al. (1998) found that the IMF power average in 1978–1982 was larger than in 1968–1972 for 150-days periodicity.

Less certain is the existence of the periodicity of 154 days in solar activity cycles prior to cycle 21. Evidence for the 154-day periodicity during cycle 19 is debated; it has been detected in the sunspot blocking function (Lean and Brueckner, 1989) and solar proton events (Gabriel et al., 1990), but not in comprehensive flare index (Bai, 1987; Kile and Cliver, 1991). Bai (1987) also found that the dominant period for flare occurrence in cycle 19 was that of 51 days and not that one of 154 days. If the 154-day periodicity observed mainly in cycle 21 is a deep-seated characteristic of solar activity and not a random transient effect, it means that its amplitude varies greatly from cycle to cycle. The same result is also obtained from the work of Valdés-Galicia et al. (1996). It means that this fluctuation appeared more easily in one odd cycle, when the cosmic ray particles penetrate the heliosphere through the current sheet than in the even one when they drift into the heliosphere from the polar latitudes.

All the above-mentioned suggest that the 154-days periodicity may be a fundamental characteristic of the Sun although the cause of this periodicity remains unknown. The spectra contain lines (or show power at frequencies) consistent with a model in which the periodicity is caused by differential rotation of active zones (Gabriel et al., 1990) and a model in which it is related to beat frequencies between solar oscillations, as proposed by Wolff (1983). Such periodic behaviour was also interpreted by Wolff (1992), as due to periodic sources located in the solar interior caused by global oscillation modes.

Table 3
Analytical expression of CR time series as a function of quasi-periods (in days)

$$A^{cal} = 1985 + a_1 \sin[(2\pi/130)(T - Ts)] + a_2 \sin[(2\pi/100)(T - Ts)] + a_3 \sin[(2\pi/70)(T - Ts)] + a_4 \sin[(2\pi/50)(T - Ts)] + a_5 \sin[(2\pi/32)(T - Ts)] + a_6 \sin[(2\pi/24)(T - Ts)] + a_7 \sin[(2\pi/16)(T - Ts)] + a_8 \sin[(2\pi/10)(T - Ts)] + a_9 \sin[(2\pi/5)(T - Ts)],$$

where $Ts < T < Te$, Ts (start time) and Te (end time) express the number of days after 1/11/81

		Ts	Te			Ts	Te
a_1	225.000	95	225	a_9	79.000	273	280
a_2	239.000	1	95		63.000	390	397
a_3	104.879	192	226		74.000	397	405
	174.000	464	498		98.402	257	264
a_4	141.145	70	94		22.521	423	430
a_5	6.990	158	192		−29.000	505	411
	−94.217	23	52		−25.000	411	417
	139.000	436	464		−22.105	264	270
a_6	68.000	284	310		21.726	283	289
	85.000	340	366		19.385	310	316
	99.000	366	390		−35.000	350	356
	114.163	462	486		53.114	384	390
	83.000	425	436		14.500	408	414
a_7	−90.302	52	70		12.000	414	417
	88.891	104	112		28.000	228	233
	41.585	122	138		51.000	248	253
	59.804	302	310		7.000	324	329
	133.490	94	104		−27.462	145	150
	168.993	1	12		20.000	242	247
a_8	53.000	233	246		−22.651	316	321
	51.377	361	374		20.377	356	361
	−239.000	253	264		39.100	437	442
	−38.197	442	453		10.464	458	462
	48.000	314	324		−26.000	310	314
	53.697	112	122		59.000	417	422
	−17.699	150	158		−30.389	141	145
	23.370	230	240		8.000	226	230
	69.213	250	255		−35.657	324	328
	−35.627	374	384		−10.997	332	336
	44.000	264	273		−14.623	346	350
	42.000	331	340		46.107	402	406
	28.339	12	21				
	−28.258	489	498				
	−19.504	292	300				
	32.499	338	346				

Bai and Sturrock (1991, 1993) reported that besides the 154-day periodicity, those of 51, 78, 104 and 129 days are often detected in solar activity and these periods are very close to integral multiples (2, 3, 4, 5, 6) of 25.8 days. These periodicities are not continuously in operation, but have a rather episodic nature. The period of 25.8 days might be a fundamental period of the Sun while those of 51, 77, 103, 129 and 154 days are its sub-harmonics. The cause of 154-day periodicity still remains unknown, but a suggestion that it was related to enhanced flare activity in certain longitude bands has been given.

Pap et al. (1990), also, reported that 51-day and 150–157-day periods are more pronounced in those solar data which are related to a strong magnetic field. In the analysis of the longitudinal distribution of flares in rotating coordinate system, Bai and Sturrock (1993) proposed that the rotation of a

Table 4
Quasi-periods (P) in days, standard deviation (σ) and the accuracy (Ac) between observed and computed values by the SA steps according to the relation 1 (see Tables 1–3)

Steps	P	σ	Ac
F50 time series			
1st	160, 70, 50, 26, 21, 5	0.84	10%
2nd	70, 50, 32, 26, 21, 16, 10, 5	0.36	20%
3rd	32, 26, 21, 16, 10, 5	0.25	42%
4th	21, 16, 10, 5	0.13	68%
F150 time series			
1st	168, 42	2.21	19%
2nd	98, 70, 42, 28	0.69	41%
3rd	42, 28, 21	0.34	71%
CR time series			
1st	130, 100, 70, 32, 24, 10, 5	48.52	98%
2nd	70, 50, 32, 24, 16, 10, 5	23.69	99%

structure in the Sun might play the role of the clock mechanism for the fundamental period. Bai (1994) reported a 51-day periodicity, the second sub-harmonic, in the occurrence rate of major flares (X-ray class $\geq$M3.0) that had been in operation during the time interval from May 4, 1991 to November 15, 1992.

Das et al. (1996) reported a periodicity of 74 days in the time series of the solar flares proton fluence measured in the cycle 22 in the three ranges of energy (>1 MeV, >10 MeV and >100 MeV), indicating the intimate relationship of proton emission with solar activity.

Moreover, several authors have studied the frequency distribution of the galactic cosmic-ray fluctuations in the range $10^{-6}-10^{-4}$ Hz (Attolini et al., 1974). The result of these works is the relationship between the general characteristics of power spectral density of cosmic ray flux and the random component of the IMF with indication of a change below 5×10^{-7} Hz.

Kudela et al. (1991) carried out a power spectral analysis of cosmic rays recorded by Neutron Monitors at Calgary and Deep River covering a wide range of frequencies from 3×10^{-9} Hz to 6×10^{-6} Hz (periodicities from 2 days to 11 years) during the epoch 1965–1989 revealed different behaviour of the power spectral density for the three ranges of frequency domains. They reported that the large cosmic-ray periodical variations might have been caused by possible heliospheric cavity oscillations from the heliospheric boundary at a distance of 110–130 AU corresponding to $T\approx20$ months. The peaks on the power spectra between 6 and 18 months could be due to the transient effects resulting in different quasi-periodical variations during different epochs.

Recently, Kudela et al. (2002) presented wavelet transform results from the time series of daily averages of the nucleonic intensity recorded by Neutron Monitors at four different cut-off rigidities over a period of four solar cycles and described the power spectral density temporal evolution at the periodicities of 150–160 days, ~1.3 years and ~1.7 years. They indicated that the quasi periodicity of about 150 days is not stable and it ranges from 140 days to more than 200 days appearing usually just after the solar maxima. This periodicity is appeared only in the 21st solar maximum (odd cycle) which is consistent with our results.

El-Borie and Al-Thoyaid (2001) investigated various CR rigidities over a wide range of frequencies from 2.3×10^{-8} Hz to 5.8×10^{-6} Hz (periodicities from 2 to 500 days), over the period 1964–1995 and indicated several periods: a broad peak near 250–300 days (0.7–0.8 year), narrower peaks at 27 days and its two first harmonics, and several peaks greater than 1 month. They showed different behaviours for the periods of solar activity maximum and minimum.

Joshi (1999) noted that the power spectrum analysis of cosmic rays for the years 1989–1991, maximum of the cycle 22, shows a periodicity of 170 days. This periodicity is related to a strong magnetic field, as cosmic rays are associated with magnetic clouds (Badruddin et al., 1986) that are associated with shocks, coronal mass ejections and geomagnetic storms. On the other hand, short-term cosmic ray changes, the so-called Forbush decreases, are mainly due to shocks. Shocks in turn are mainly associated to fast coronal mass ejection, although flares and transient coronal holes may contribute with some.

However, as far as the cosmic ray long-term changes are concerned, there is a debate between those that attribute these changes to the global changes of the Sun's magnetic field, where transients do not play an important role (Cane et al., 1999) and those that claim that coronal mass ejections also

Table 5
Periods determined by the different spectral methods

Methods		Periods in days					
Cosmic-ray intensity (CR time series)							
FFT		140±14		88±10	50±4	27±2	
(>95%)						32±2	
SA		130	100	70	50	32	16 5
(99%)						24	10
F50 time series							
FFT		154±50		67±15	40±5	24±3	17±2 12±1
(>95%)							
MESA	$F = 84$		100±25			25±3	18±2 12±1 8±1
	$F = 94$			67±15	52±5	25±3	18±2 12±1 8±1
SA		160		70	50	32	21 16 10
(68%)						26	5
F150 time series							
FFT		174±60	100±10	63±6	41±3	28±3	
(>95%)							
MESA F=35		199±36	107±9	60±3	45±5	28±2	18±2
SA							
(71%)		168	98	70	42	28	21
Occurrence rate of hard X-ray solar flares with energy >50 keV (Venera 13, 14 and SMM)							
FFT		140±25		77±10	50±2	(26±1)	(21±1)
(>95%)					36±2	32±1	
SA		140	105	70	49	28	21
(87%)					35		
Occurrence rate of hard X-ray solar flares with energy >150 keV (Venera 13, 14 and SMM)							
SA		154	105	70	49	28	21
(86%)					35		
FFT		140±25		80±10	50±5	(26±1)	(21±1)
(>95%)					35±5		

NOTE: In parenthesis are periodicities with low significant level (75%), according to Kolmogorov–Smirnov test. The error bar ± refers to the peaks dispersion corresponding to the FWHM of FFT and MESA spectrum peaks.

produce these changes (Caballero and McDonald, 2003). In any case it is clear, at least for the moment, that flares are not influencing the cosmic rays directly.

5. Conclusions

An investigation is carried out regarding the problem of galactic cosmic-ray modulation by solar flares with high enough energy release associated by strong variations in the solar magnetic field. The solar flares, with hard X-ray emission, are expressed by their fluence, that is a more convenient way to compare with the cosmic-ray intensity.

It is known that no close relationship exists between soft X-ray flare indices and cosmic ray intensity modulation (Storini et al., 1995). Therefore, it would be of interest to examine whether cosmic-ray data carry similar fluctuations with those ones of hard X-ray solar flares. Many authors characterized the examined time period as an interesting period with the presence of a number of strong solar flares, although it is only a short time interval (1981–1982).

The spectral analysis of daily means of cosmic-ray intensity recorded at Neutron Monitor energies in the

frequency range $10^{-8}-10^{-7}$ Hz from November 1981 to March 1983 has permitted us to present a comprehensive description of the behavior of spectral density distributions in an interval of periodicities ranging from 154 to 7 days. These variations grouped in 152, 100, 70, 50, 32, 27 and 14 days seems to be well established in cosmic-ray data during this time period. Except for the well-known 27-day periodicity and the one of 152 days, the presence of others was not conflicting with earlier appearances in cosmic-ray intensity.

The same analysis applied on the time series of the solar hard X-ray flares with energy higher than 50 and 150 keV that have been recorded by Venera 13, 14 space-probes during the same time interval gave similar variations.

Similar periodicities established in the cosmic-ray intensity and in the flare activity indicate the possible link between them. Cane et al. (1999) noted that the cosmic ray density is a mirror image of the magnitude of the IMF. They suggested that global changes in the Sun's magnetic field are more important for long-term modulation than magnetic field enhancements resulting from the emerging of high-speed flows and coronal mass ejections in the outer heliosphere. It is known that the close relation between flare activity and global changes of the Sun's magnetic field that affect the IMF variations. According to Valdés-Galicia and Mendoza (1998) the characteristic times of several features on the Sun related with magnetic flux emergence and transport, such as, sunspots, Ha flares, magnetic features etc are compatible with the dominant fluctuation of cosmic ray intensity of 20 months.

In conclusion, the study of the spectral behaviour of the cosmic-ray data and the flare-related data during maxima of other solar cycles, which do not resemble the characteristic 1981–83 interval, may be interpreted by some non-stationary processes affecting the cosmic ray/hard X-ray parameters relationship.

Hard X-ray solar flares (>50 keV) are good indicators of relevant large-scale coronal changes. If this hypothesis is true, solar hard X-ray flares could be regarded as a proxy data set to account for peculiar solar-induced effects in the heliosphere. Once again, the investigation of cosmic-ray variations provides a unique tool to derive information about the three-dimensional configuration of the IMF in the heliosphere which will be very useful to the studies of the space weather forecast.

Acknowledgements

We thank our colleagues for kindly providing cosmic ray data as well as solar hard X-ray flares used in this work. We also thank the anonymous referee for valuable comments. The present work is supported by the grant 70/4/6255 of the Ministry of Development of the General Secretariat of Research and Technology concerning the Greek–Russian collaboration. Thanks are also due to the Special Research Account of Athens University for supporting these researches.

References

Antalova, A., 1994. Adv. Space Sci. 14, 721.
Antalova, A., 1997. Adv. Space Sci. 20, 111.
Antalova, A., Kudela, K., Storini, M., 2000. ESA SP-463, 281.
Atac, T., 1987. Ap&SS 135, 201.
Attolini, M.R., Cecchini, S., Galli, M., 1974. NCimC 7, 413.
Attolini, M.R., Cecchini, S., Galli, M., 1987. Ap&SS 134, 103.
Bai, T., 1987. ApJ 318, L85.
Bai, T., 1994. SoPh 150, 385.
Bai, T., Cliver, E.W., 1990. ApJ 363, 299.
Bai, T., Sturrock, P.A., 1991. Nature 152, 360.
Bai, T., Sturrock, P.A., 1993. ApJ 409, 476.
Barat, C., Vedrenne, G., Vilchinskaya, A., Dyachkov, A., Zenchenko, V., Kurt, V., Yurovitskaya, E., 1987. Preliminary data from Solar Hard X-Ray Monitor on Venera 13, 14. Soviet Geophys. Com., Academy of Sciences of the USSR.
Badruddin, Yadav, K.S., Yadav, N.R., 1986. SoPh 105, 413.
Berryman, J.G., 1978. Geophysics 43, 1383.
Bogart, R.S., Bai, T., 1985. ApJ 229, 151.
Caballero, J.A., McDonald, F.B., 2003. Adv. Space Res., in press.
Cane, H.V., Richarson, I.G., von Rosenvinge, T.T., 1998. J. Geophys. Res. 25, 4437.
Cane, H.V., Wibberenz, G., Richarson, I.G., von Rosenvinge, T.T., 1999. Geophys. Res. Lett. 26, 565.
Chatfield, C., 1984. The Analysis of Time-series. an Introduction, 3rd Edition. Chapman and Hall, London.
Das, T.K., Nag, T.K., Chatterjee, T.N., 1996. SoPh 168, 385.
Dorman, L.I., Ptuskin, V.S., 1981. Ap&SS 79, 397.
El-Borie, M.A., Al-Thoyaid, S.S., 2001. Proc. 27th ICRC, Hamburg, 3877.
Filisetti, O., Musino, V., 1982. Revista Brasiliera de Fisica 12, 599.
Forbush, S.E., 1958. J. Geophys. Res. 63, 651.
Gabriel, S., Evans, R., Feynman, J., 1990. SoPh 128, 415.

Ichimoto, K., Kubato, J., Suzuki, M., Tohmura, I., Kurokawa, H., 1985. Nature 316, 422.
Jakimiec, M., Storini, M., Antalová, A., 1997. Adv. Space Sci. 20, 111.
Joshi, A., 1999. SoPh 185, 397.
Kile, J.N., Cliver, E.W., 1991. ApJ 370, 442.
Kleczek, J., 1952. Bubl. Centr. Inst. Astron. No. 22, Prague.
Kudela, K., Ananth, A.G., Venkatesan, D., 1991. J. Geophys. Res. 96, 15871.
Kudela, K., Rybak, J., Antalova, A., Storini, M., 2002. SoPh 205, 165.
Lean, J.L., Brueckner, G.E., 1989. ApJ 337, 568.
Liritzis, I., Preka-Papadema, P., Petropoulos, B., Banos, C., Kostopoulos, T., 1999. P&SS 47, 469.
Liritzis, I., Preka-Papadema, P., Petropoulos, B., Kurt, V., Adrianopoulos C., 2001. Proc. 4th Astron. Conf., 207
Liritzis, I., Xanthakis, J., Petropoulos, B., Banos, C., Sarris, E., 1994. P&SS 43 (9), 1067.
Liritzis, I., 1994. SoPh 161, 29.
Longair, M.S., 1992. High-Energy Astrophysics. Cambridge University Press, Cambridge.
Maravilla, D., Lara, A., Valdés-Galicia, J.F., Mendoza, B., 2001. SoPh 203, 27.
Mavromichalaki, H., Vassilaki, A., Marmatsouri, E., 1988. SoPh 115, 345.
Mavromichalaki, H., Marmatsouri, E., Vassilakli, A., 1990. SoPh 125, 409.
Mavromichalaki, H., Marmatsouri, E., Vassilakli, A., 1995. Ap&SS 232, 315.
Mavromichalaki, H., Belehaki, A., Liritzis, J., 1989. EM&P 4, 1.
Mavromichalaki, H., Belehaki, A., Serdari, V., 1991. Ap&SS 180, 173.
McIntosh, P.S., 1992. In: Harvey, K.L. (Ed.), The Solar Cycle, ASP Conf. Proc. 27, San Francisco, CA, p. 14.
Nakai, H., Kamide, Y., 1994. J. Geophys. Res. 99, 23747.
Okhlopkov, V.P., Okhlopkova, L.J., Charakhyan, T.N., 1986. Geomagn. and Aeronomy 26, 19.
Ozgüc, A., 1989. Ap&SS 162, 123.
Ozgüc, A., Atac, T., 1994. SoPh 150, 339.
Pap, J., Tobiska, W.K., Bouwer, S.D., 1990. SoPh 129, 165.
Rieger, E., Share, G.H., Forrest, D.J., Kanbach, G.H., Reppin, C., Chupp, E.L., 1984. Nature 312, 623.
Rybak, J., Antalova, A., Storini, M., 2000. ESA SP–463, 419.
Saporta, G., 1990. Probabilités, Analyse des Données et Statistique, Editions Technip., Paris.
Schwenn, R., 1983. NASAC 2280, 489.
Smith, E.J., 1990. J. Geophys. Res. 95, 18741.
Storini, M., Antalová, A., Jakimiec, M., 1995. J. Geomagn. Geoelectr. 47, 1085.
Valdés-Galicia, J.F., Perez-Enriquez, R., Otaola, J., 1996. SoPh 167, 409.
Valdés-Galicia, J.F., Mendoza, B., 1998. SoPh 1178, 1183.
Webb, D.F., Howard, R.A., 1994. J. Geophys. Res. 99, 4201.
Wolff, C.L., 1983. ApJ 264, 667.
Wolff, C.L., 1992. SoPh 142, 187.
Xanthakis, J., Mavromichalaki, H., Petropoulos, B., 1989. SoPh 122, 345.
Xanthakis, J., Liritzis, I., Tzanis, E., 1995. EM&P 66, 253.